



ON THE ROLE OF THE LIFT FORCE IN TURBULENCE SIMULATIONS OF PARTICLE DEPOSITION

Q. WANG¹, K. D. SQUIRES¹, M. CHEN² and J. B. McLAUGHLIN²

¹Department of Mechanical Engineering, 209 Votey Building, University of Vermont, Burlington, VT 05405, U.S.A.

²Department of Chemical Engineering, Clarkson University, Potsdam, NY 13699, U.S.A.

(Received 29 January 1996; in revised form 5 February 1997)

Abstract—Most calculations of particle deposition in turbulent boundary layers have been performed using an equation of motion in which the form for the lift force is that in a linear shear flow for a particle far from any boundaries, the so-called Saffman formula. Both direct and large eddy simulations of particle deposition in turbulent channel flow have shown that the dependence of the deposition velocity on particle relaxation time is over-predicted using the Saffman force. Since the derivation of the Saffman force there have been more general derivations of the lift on a particle in a shear flow. In this paper an ‘optimum’ lift force is formulated which represents the most accurate available description of the force acting on a particle in a wall-bounded shear flow. The effect of the force was examined through large eddy simulation (LES) of particle deposition in vertical turbulent channel flow. The optimum force for depositing particles is approximately three times smaller than the lift obtained using the Saffman formula. LES results also show that use of the optimum force yields a dependence of the deposition velocity on particle relaxation time less than that obtained using the Saffman form and in better agreement with experimental measurements. Neglecting the lift force altogether leads to an even smaller dependence of the deposition velocity on particle relaxation time and is in better agreement with empirical relations, although the deposition rates are smaller than experimental measurements for particles with intermediate relaxation times. © 1997 Elsevier Science Ltd.

Key Words: lift force, particle deposition

1. INTRODUCTION

In an earlier work on particle deposition in vertical turbulent channel flow, Wang and Squires (1996a) found that statistical measures predicted by large eddy simulation (LES) were in good agreement with the direct numerical simulation (DNS) results of McLaughlin (1989). In Wang and Squires (1996a) and McLaughlin (1989), as well as the majority of calculations of particle deposition in turbulent boundary layers, the effect of shear-induced lift as derived by Saffman (1965, 1968) is included in the particle equation of motion (e.g. see Kallio and Reeks 1989; McLaughlin 1994). The bulk of this work has demonstrated that the Saffman lift force is important near the wall, i.e., in the viscous sublayer, and enhances deposition (McLaughlin 1989; Wang and Squires 1996a).

Saffman (1965, 1968) derived the force on a particle due to velocity shear by considering motion far from any boundaries and in which the fluid velocity gradient is constant. Saffman assumed that Reynolds numbers defined in terms of the slip velocity, Re_s , and velocity gradient, Re_G , were small compared to unity and that $Re_s \ll Re_G^{1/2}$. However, in a DNS study of aerosol motion in a turbulent channel flow at moderate Reynolds number, McLaughlin (1991) reported that the value of Re_G is typically of order 0.04 whereas Re_s is of order unity, indicating that Re_s is not small compared to $Re_G^{1/2}$. The fact that the Saffman formula also does not take into account the influence of the wall further limits its applicability. Consequently, it should be expected that the lift force predicted using the Saffman formula will not be accurate near solid boundaries. In fact, the DNS results of McLaughlin (1989) and LES predictions of Wang and Squires (1996a) show that the dependence of the deposition rate on particle relaxation time is over predicted using the Saffman lift force (see figure 1).

There have been several other investigations into more general forms of shear-induced lift on a particle as well as corrections due to the presence of the wall (e.g. see Vasseur and Cox 1977; Cox and Hsu 1977; McLaughlin 1991, 1993 and Cherukat and McLaughlin 1994). McLaughlin (1991) analyzed the lift force on a particle in an unbounded shear flow and modified the Saffman formula by removing the restriction that $Re_p \ll Re_g^{1/2}$. It was found that the resulting force in some cases is much smaller in magnitude than the Saffman formula. Vasseur and Cox (1977) considered the force acting on a particle in a uniform flow between two parallel walls and derived a form for the force due to the presence of the wall so long as the wall lies in the outer region of the disturbance created by the particle. The force obtained by Vasseur and Cox (1977) can be considered a correction to the lift due to the wall and is valid when the Reynolds number based on the distance of the particle from the wall and a characteristic flow velocity is large compared to unity. Cox and Hsu (1977) considered the force acting on a particle in a shear flow and derived the lift force for the case in which the wall lies in the inner region of the particle disturbance. All the above forces assume the distance between the particle and wall is much larger than the particle radius. Cherukat and McLaughlin (1994) obtained an expression for the lift force on a particle which is valid when the distance between the particle and wall are comparable to the particle radius.

In a later work, McLaughlin (1993) derived a form of the lift force due to the presence of the wall which provides a connection between the analyses of Vasseur and Cox (1977) and Cox and Hsu (1977). By merging the formula derived by Cherukat and McLaughlin (1994), applicable close to a boundary, together with the formula in McLaughlin (1991), Vasseur and Cox (1977), Cox and

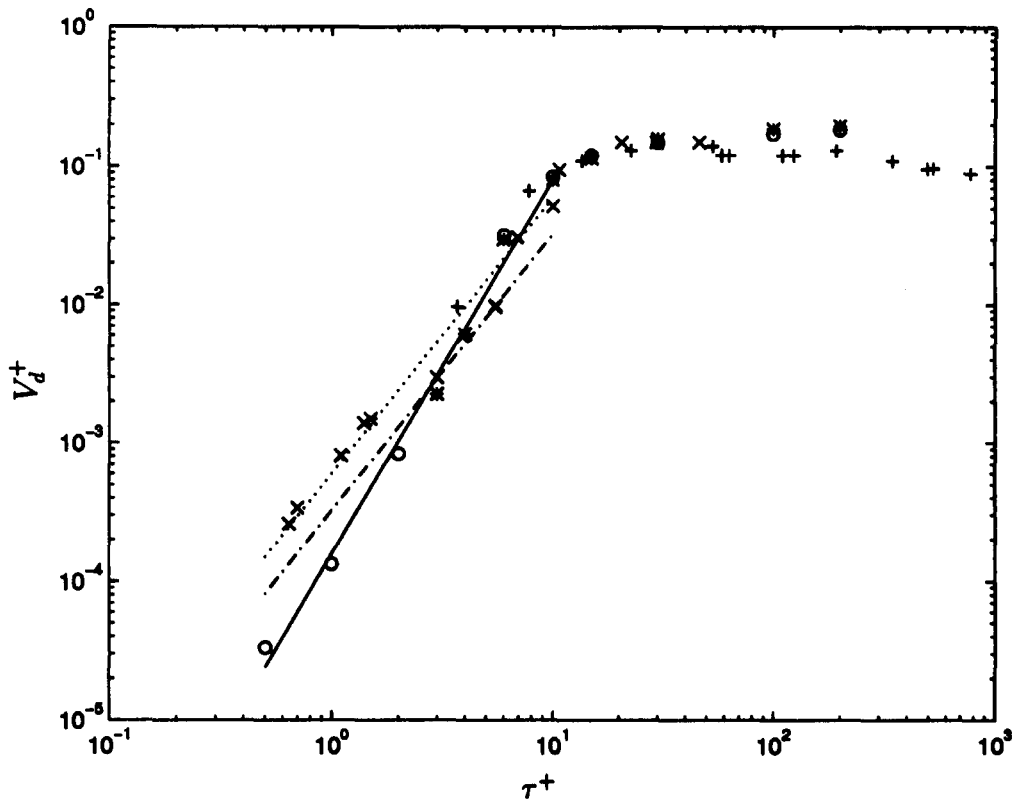


Figure 1. Particle deposition rate in turbulent channel flow from Wang and Squires (1996a). The deposition velocity is denoted V_d^+ , ρ is the ratio of particle to fluid density, and τ is the particle relaxation time. In the figure and throughout this work the + subscript is used to express quantities in terms of wall variables. LES calculations performed using Saffman lift force, $\rho = 713$ $V_d^+ = 0.0006(\tau^+)^2$ (Liu and Agarwal 1974); — — — $V_d^+ = 0.000325(\tau^+)^2$ (McCoy and Hanratty 1977). LES: \circ $Re_p = 180$; $*$ $Re_p = 1000$; — — — least-squares fit of LES results; Liu and Agarwal (1974) (Reynolds numbers based on pipe diameter and average velocity): \times $Re_p = 10,000$; $+$ $Re_p = 50,000$. LES predictions of the deposition velocity exhibit a stronger dependence on relaxation time than measured in experiments. A least-squares fit of the LES predictions yields a dependence of the deposition rate on particle relaxation time of $\tau^{+2.72}$.

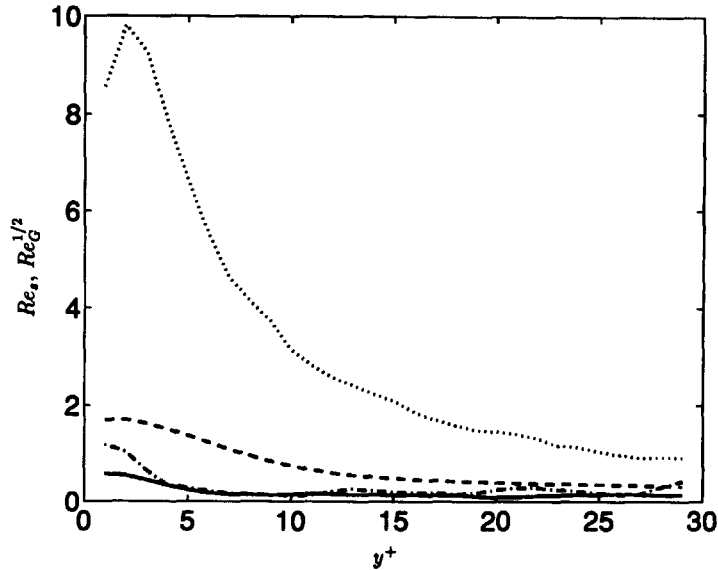


Figure 2. Wall-normal profiles of the Reynolds numbers Re_s and $Re_G^{1/2}$ averaged over particles which deposit. $\tau^+ = 6$: — $Re_G^{1/2}$; - - - Re_s ; $\tau^+ = 100$: ···· $Re_G^{1/2}$; ···· Re_s .

Hsu (1977), and McLaughlin (1993) for the lift force acting on a particle further away from the wall, one obtains a force applicable near boundaries and also appropriate for regimes much less restrictive than the Saffman formula. It should be expected that more accurate forms of the lift force acting on a particle will improve predictions of particle deposition in turbulent boundary layers. In this paper an ‘optimum’ lift force is formulated which represents the most accurate available description of the force acting on a particle in a wall-bounded shear flow. The force is then implemented in large eddy simulations of particle deposition in vertical turbulent channel flow. An overview of previous investigations of the lift force acting on a particle in a wall-bounded shear flow and formulation of the ‘optimum’ force is presented in section 2. A discussion of the simulations is presented in section 3 together with LES results. A summary of the work may be found in section 4.

2. BACKGROUND

The form for the lift force employed in previous studies and used by Wang and Squires (1996a) is that derived by Saffman (1965, 1968)

$$F_2 = -6.46 \mu a^2 U_s \operatorname{sgn}(G) \left[\frac{|G|}{\nu} \right]^{1/2}, \quad [1]$$

where a is the particle radius, μ is the dynamic viscosity, ν is the kinematic viscosity, $G = du_1/dy$ is the wall-normal gradient of the streamwise fluid velocity, and $U_s = v_1 - u_1$ is the instantaneous streamwise velocity difference between particle and fluid (defined at the particle center). It is important to note that [1] as well as the other forms for the lift force considered in this section are based on singular or regular perturbation solutions of the Navier–Stokes equations. Thus, these solutions are strictly applicable when the Reynolds numbers are smaller than unity. Furthermore, in the derivation of the Saffman force (1) the Reynolds number based on the slip velocity, $Re_s = |U_s|d/\nu$ is assumed to be much smaller than that defined in terms of the velocity shear, $Re_G^{1/2} = [|G|d^2/\nu]^{1/2}$, where $d = 2a$ is the particle diameter. However, McLaughlin (1991) showed that, on average, $Re_G^{1/2}$ is smaller than Re_s for aerosol transport in a turbulent channel flow. Figure 2 shows wall-normal profiles of Re_s and $Re_G^{1/2}$ from the LES calculations of Wang and Squires (1996a) for two particle relaxation times averaged over particles which deposit. It is clear that these Reynolds numbers are dependent upon both particle relaxation time and distance from the wall.

The figure also shows that the condition $\text{Re}_s \ll \text{Re}_G^{1/2}$, assumed in the derivation of [1], is violated. For particles with $\tau^+ = 100$, the value of Re_s can be as much as five times larger than $\text{Re}_G^{1/2}$ while the difference is smaller for particles with smaller τ^+ . The maximum values of Re_s are 25 and 2.5 for $\tau^+ = 100$ and $\tau^+ = 6$, respectively, while the maximum $\text{Re}_G^{1/2}$ is 3.5 and 0.8.

McLaughlin (1991) relaxed the Reynolds number restriction in the Saffman formula and derived an expression for the lift force

$$F_2 = -\frac{9}{\pi} \mu a^2 U_s \text{sgn}(G) \left[\frac{|G|}{\nu} \right]^{1/2} J^n, \quad [2]$$

where the function J^n is dependent upon the dimensionless parameter

$$\epsilon = \text{sgn}(GU_s) \frac{\text{Re}_G^{1/2}}{\text{Re}_s} = \text{sgn}(G) \frac{\sqrt{|G|\nu}}{U_s}. \quad [3]$$

Since the general expression for J^n is rather complicated, the value is tabulated for $\epsilon \sim O(1)$ in McLaughlin (1991). Analytical forms for asymptotically small and large ϵ are also derived in McLaughlin (1991)

$$J^n = -32\pi^2 |\epsilon|^5 \ln(1/\epsilon^2), \quad |\epsilon| \ll 1, \quad [4]$$

$$J^n = 2.255 - 0.6463/\epsilon^2, \quad |\epsilon| \gg 1. \quad [5]$$

Note that, for $|\epsilon| \rightarrow \infty$, $J^n = 2.255$ and the force is identical to the Saffman formula [1]. Figure 3 shows the function J^n vs ϵ , where J^n is calculated using [4] for $\epsilon < 0.025$ and [5] for $\epsilon > 5$ while linear interpolation from the values in table 1 in McLaughlin (1991) is used to obtain J^n for $0.025 \leq \epsilon \leq 5$. Also shown in the figure is the Saffman formula [1]. It is clear that the two functions coincide only for large $|\epsilon|$, i.e. $\text{Re}_s \ll \text{Re}_G^{1/2}$, which Saffman assumed in deriving [1]. For smaller $|\epsilon|$, however, the lift force obtained from [1] is much larger than that from McLaughlin (1991). In fact, figure 3 shows that for $\epsilon \sim 0.15$ the sign of the Saffman force is also incorrect.

Both [1] and [2] were derived for a particle in a shear flow away from walls. A force on a particle due to the presence of a wall and valid at distances far from the wall was derived by Vasseur and Cox (1977). Vasseur and Cox considered the force on a particle in a quiescent flow field bounded by two walls. Defining the distance between the walls as L and that between the particle and the

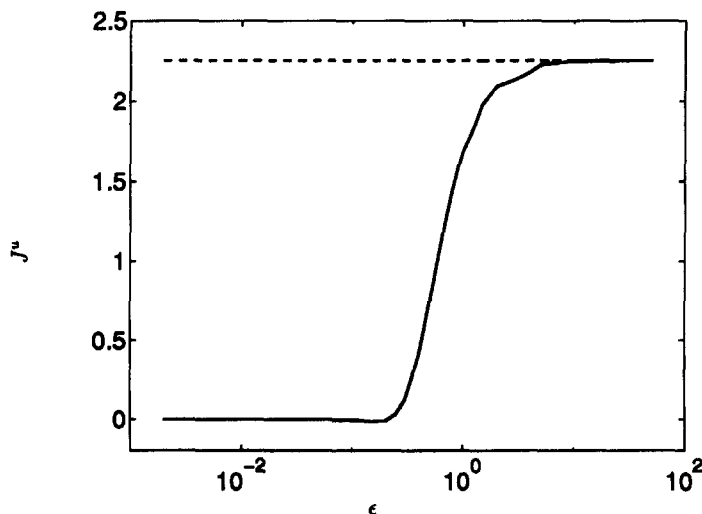


Figure 3. Profile of J^n . — McLaughlin (1991); - - - Saffman (1965, 1968).

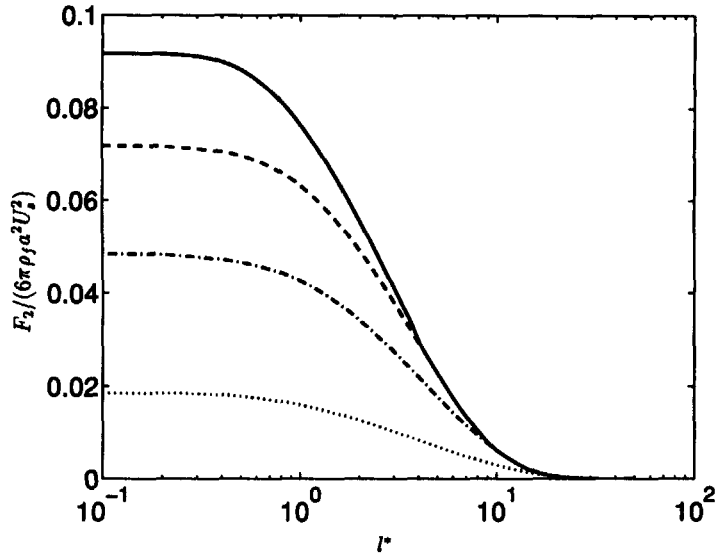


Figure 4. Lift force from Vasseur and Cox (1977), [6]. — $l/L = 0$; - - - $l/L = 0.25$; - · - $l/L = 0.35$; . . . $l/L = 0.45$.

wall as l , the lift force derived by Vasseur and Cox is

$$\begin{aligned} \frac{F_2}{6\pi\rho_f a^2 U_s^2} = & \frac{3}{2\pi} \int_{-\infty}^{\infty} \int_{-\infty}^{\infty} \frac{ik_1}{\lambda} \{ \cosh[(t+q)l^*] - \cosh[(t-q)l^*] \\ & + \cosh[(t-q)(L^* - l^*)] - \cosh[(t+q)(L^* - l^*)] \\ & + \sinh(qL^*)\sinh[t(L^* - 2l^*)] + \sinh(tL^*)\sinh[q(L^* - 2l^*)] \} dk_1 dk_2, \end{aligned} \quad [6]$$

where $l^* = l|U_s|/\nu$, $L^* = L|U_s|/\nu$, $q = \sqrt{k_1^2 + k_2^2}$, $t = \sqrt{k_1^2 + k_2^2 + ik_1}$, ρ_f is the density of the fluid and

$$\lambda = 4tq - (t+q)^2 \cosh[(t-q)L^*] + (t-q)^2 \cosh[(t+q)L^*]. \quad [7]$$

For $l/L \rightarrow 0$, [6] becomes

$$\frac{F_2}{6\pi\rho_f a^2 U_s^2} = \frac{3}{4\pi} \int_{-\infty}^{\infty} \int_{-\infty}^{\infty} \frac{t+q}{t-q} [e^{-qt^*} - e^{-it^*}]^2 dk_1 dk_2. \quad [8]$$

Shown in figure 4 is the lift force [6] for various values of the distance l^* and L^* . Only the values for l/L between 0 and 0.5 are shown since the force is symmetric about the centerline between the walls. Figure 4 shows that [6] is always positive (i.e. directed away from the wall). For particles at the channel centerline, $l/L = 0.5$ and [6] yields zero force. It should also be noted that the force [6] derived by Vasseur and Cox (1977) is applicable when the wall lies in the outer region of the particle disturbance and for which there is no shear in the flow field. Cherukat and McLaughlin (1990) have shown that the form of the lift force derived by Vasseur and Cox was in good agreement with their experimental measurements for particle Reynolds numbers up to three. Cox and Hsu (1977) derived a formula for the inertial migration velocity v_m of a spherical particle in a vertical linear shear flow

$$v_m = \frac{3}{32} \frac{aU_s^2}{\nu} - \frac{11}{64} \frac{GaU_s l}{\nu}. \quad [9]$$

The corresponding lift force, including both the shear- and wall-induced parts, can be obtained from [9]

$$F_2 = \frac{3}{32} \pi \rho_f a^2 U_s (6U_s - 11Gl). \tag{10}$$

Note that [10] is valid when the wall lies in the inner region of the particle disturbance.

Each of the forces discussed above are derived by assuming that the distance between the particle and wall are much greater than the particle radius, i.e. $l/a \gg 1$. Cherukat and McLaughlin (1994) derived a form of the lift force which is applicable when the distance between the particle and wall is comparable to the particle radius

$$\begin{aligned} \frac{F_2}{\rho_f a^2 U_s^2} &= 1.7716 + 0.2160\kappa - 0.7292\kappa^2 + 0.4854\kappa^3 \\ &\quad - (3.2397\kappa^{-1} + 1.1450 + 2.0840\kappa - 0.9059\kappa^2)\Lambda \\ &\quad + (2.0069 + 1.0575\kappa - 2.4007\kappa^2 + 1.3174\kappa^3)\Lambda^2, \end{aligned} \tag{11}$$

where $\kappa = a/l$ and the nondimensional shear is $\Lambda = aU_s/G$. If the slip velocity $U_s = 0$, the velocity scale U_s should be replaced by aG (see Cherukat and McLaughlin 1994). Note that [11] is valid for distances l such that $a < l \ll \min\{L_s, L_G\}$, where $L_s = \nu/|U_s|$ is the Stokes lengthscale and $L_G = \sqrt{\nu/|G|}$ the Saffman lengthscale. Note also that [11] reduces to [10] from Cox and Hsu for small values of κ (i.e. $l \gg a$). Shown in figure 5 is the force [11] as a function of shear and distance from the wall. It is clear that when $\Lambda < 0$ (i.e. G and U_s having opposite sign), the lift force is positive and will result in motion away from the wall. On the other hand, when $\Lambda > 0$, the lift force [11] is negative for large l/a and positive for small l/a (and large Λ).

For a particle far from the wall, McLaughlin (1993) obtained a closed form solution for the lift force which provides a connection between the various limiting cases considered by previous investigators and outlined above. The resulting expression for the lift takes the form

$$F_2 = -\frac{9}{\pi} \mu a^2 U_s \operatorname{sgn}(G) \left[\frac{|G|}{\nu} \right]^{1/2} J. \tag{12}$$

The function J is comprised of two components, $J = J^u + J^w$, where J^u corresponds to the shear-induced lift in an unbounded flow and J^w is the correction due to the presence of a wall. The

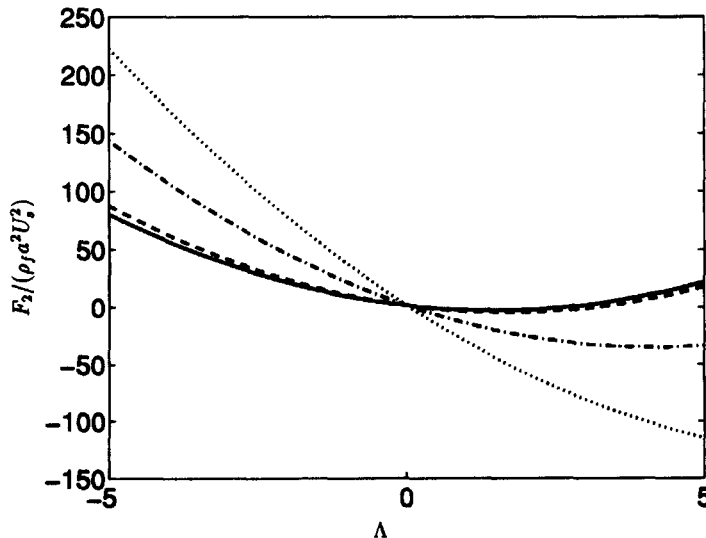


Figure 5. Lift force from Cherukat and McLaughlin (1994), [11]. — $l/a = 1.1$; - - - $l/a = 1.5$; - · - $l/a = 5.0$; · · · $l/a = 10.0$.

Table 1. Regions of applicability of optimum lift force. Tables refer to those in McLaughlin (1993)

	$ \epsilon < 0.2$	$0.2 \leq \epsilon \leq 2$	$ \epsilon > 2$
$l^+ \leq \min\{1, L_s/L_G\}$	[11]	[11]	[11]
$\min\{1, L_s/L_G\} \leq l^+ \leq 0.1$	[15]	[15] or [14]	[14]
$\max\{0.1, \min\{1, L_s/L_G\}\} \leq l^+ \leq 5$	[15]	Table 1 or 2	Table 1 or 2
$l^+ \geq \max\{5, L_s/L_G\}$	[13]	[13]	[13]

shear-induced component J^u is that derived by McLaughlin (1991) and given in [2] (note that the Saffman formula [1] corresponds to $J^u = 2.255$, $J^w = 0$). McLaughlin (1993) derived an expression for the wall-correction part J^w of [12] which depends on ϵ and the nondimensional distance from the particle center to the wall, $l^+ = l/L_G$. McLaughlin (1993) showed that the wall-correction part of the lift force is consistent with those of Vasseur and Cox (1977) and Cox and Hsu (1977) for the regions in which each is valid. The general expression for J^w in McLaughlin (1993) is quite complicated and therefore values of J are tabulated for $|\epsilon| \geq 0.2$ and $0.01 \leq l^+ \leq 5.0$. For large l^+ McLaughlin (1993) obtained an approximate expression

$$J = J^u - \frac{1.879}{(l^+)^{5/3}}. \quad [13]$$

The function J for other cases can be obtained from the simple forms derived by other investigators. In particular, for small l^+ and large $|\epsilon|$, [10] from Cox and Hsu (1977) can be used while for small $|\epsilon|$ [6] from Vasseur and Cox (1977) is appropriate. Recasting [10] in terms of ϵ and l^+ yields

$$J = \frac{\pi^2}{16} \left(\frac{11}{6} l^+ - \frac{1}{\epsilon} \right), \quad [14]$$

while the Vasseur and Cox (1977) form (6) can be rewritten as

$$J = -\frac{2\pi^2}{3|\epsilon|} I + J^u, \quad [15]$$

where I is the two-dimensional integral of the right-hand side of [6] or [8]. The unbounded-flow part J^u has been included in [15] since the form [6] obtained by Vasseur and Cox (1977) was derived by assuming the flow is stagnant (the fluid velocity gradient G does not appear). Finally, it should again be noted that the forces from Vasseur and Cox (1977), Cox and Hsu (1977), and McLaughlin (1991, 1993) shown above are derived by assuming that the distance between the particle and the wall is much larger than the particle radius. When this condition is not satisfied [11] from Cherukat and McLaughlin (1994) should be used.

The combinations of the various lift force formula described above are the most accurate description of shear-induced lift available, including corrections for the presence of a wall, and can be considered the 'optimum' force. The various expressions in the optimum force and the range in which these expressions are applicable are summarized in table 1. The force as summarized in the table is similar to that used by Chen and McLaughlin (1995) in their direct numerical simulations of particle deposition in turbulent channel flow. However, Chen and McLaughlin (1995) base the lift solely on the distance of the particle from the wall while the optimum force in table 1 is dependent upon both l^+ and ϵ . Near the wall, Chen and McLaughlin (1995) apply [10] while [11] is used in the present study. Outside the viscous sublayer (i.e. $l^+ > 5$) the optimum force is specified according to [13] while Chen and McLaughlin (1995) used [6] from Vasseur and Cox (1977) together with the shear-induced lift [2] from McLaughlin (1991). It is also important to note that, while the objective of this paper is to examine the effect of the lift force on particle deposition, Chen and McLaughlin (1995) focused on other aspects such as the effect of a Brownian random force, particle polydispersity, and different definitions of the deposition rate.

The function J for the optimum force is shown in figure 6 for various values of ϵ , together with other lift force formula. For the profiles shown in the figure the length scale based on the slip velocity, L_s , is set to zero, i.e. the lift force [11] is not used in the figure. For large ϵ , [14] from Cox and Hsu (1977) is applied for $l^+ < 0.1$ while the values in tables 1 or 2 of McLaughlin (1993) are used for $0.1 \leq l^+ \leq 5$ and [13] is used for $l^+ > 5$. As may be observed in the figure there is a

relatively smooth merging at the junctions $l^+ = 0.1$ and $l^+ = 5$. Figure 6 indicates that for large ϵ (i.e. large velocity gradient G and/or small slip velocity U_s), the optimum force and the Saffman formula are of the same sign (though the magnitudes are quite different for l^+ near zero). For small ϵ , however, the sign of the lift force from the Saffman formula could be different from the optimum force, especially for small l^+ . The optimum lift force reduces to the Saffman form when both ϵ and l^+ are large. As is also clear from figure 6(a), for small ϵ , the optimum lift force is almost the same as that from Vasseur and Cox, and therefore in good agreement with the experimental measurements of Cherukat and McLaughlin (1990).

Hall (1988) measured the lift force acting on spheres on and near the wall of a turbulent boundary layer and it is therefore of interest to compare predictions of the lift for the optimum force to Hall's measurements. For particles on a smooth surface, Hall (1988) showed the data were well correlated by

$$F_2^+ = 20.90(a^+)^{2.31}, \tag{16}$$

for measurements in the range $1.8 < a^+ < 70$, where a^+ is the particle radius and F_2^+ is the force,

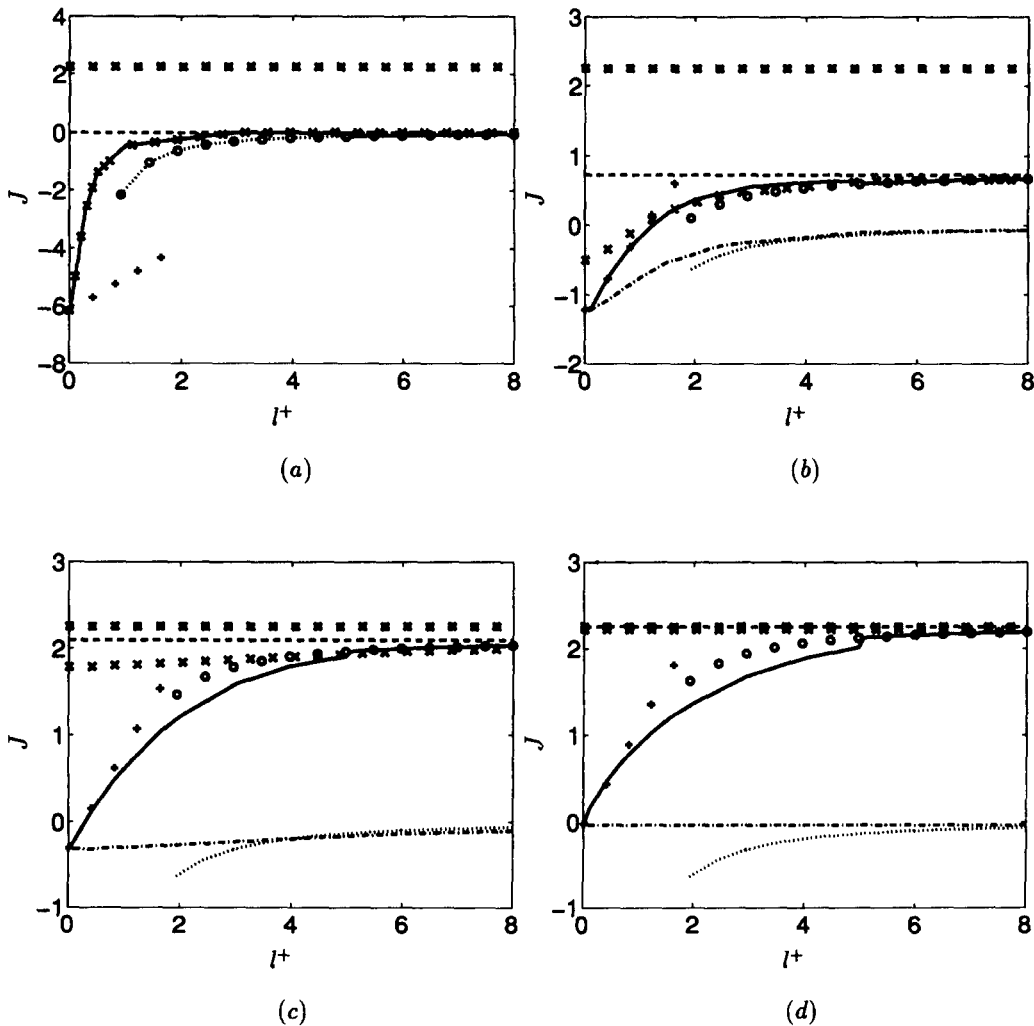


Figure 6. Comparison of J in [12] for the 'optimum' lift force to other limiting cases. (a) $\epsilon = 0.1$; (b) $\epsilon = 0.5$; (c) $\epsilon = 2.0$; (d) $\epsilon = 20.0$. — 'optimum' lift force, table 1; - - - [4] and [5] and tables (McLaughlin 1991); — · — [6] (Vasseur and Cox 1977); · · · · · $J = -1.879/(l^+)^{5.3}$ (McLaughlin 1993); + [14] (Cox and Hsu 1977); * [1] (Saffman 1965, 1968); × [15] (Vasseur and Cox 1977 and McLaughlin 1991); ○ [13] (McLaughlin 1993 and McLaughlin 1991).

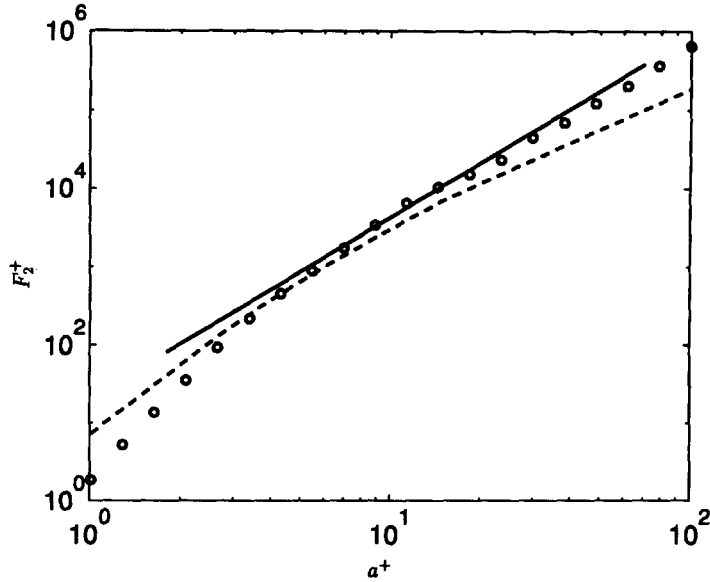


Figure 7. Comparison of the 'optimum' lift force, the Saffman force, and the correlation from Hall (1988). — [16]; O 'optimum' lift force; ---- Saffman force.

both expressed in wall units. In terms of inner variables, [12] can be rewritten as

$$F_2^+ = -\frac{9}{\pi} (a^+)^2 U_s^+ \operatorname{sgn}(G) |G^+|^{1/2} J. \tag{17}$$

Shown in figure 7 is comparison of the optimum force as well as the Saffman formula to the correlation [16] from Hall (1988). Similar to the comparison considered in Hall (1988), the streamwise mean slip velocity used for calculating the force in figure 7 is prescribed as

$$U_s^+ = \begin{cases} l^+ & l^+ < 5 \\ -30.5 + 5.0 \ln l^+ & 5 \leq l^+ < 30 \\ 5.5 + 2.5 \ln l^+ & l^+ \geq 30. \end{cases} \tag{18}$$

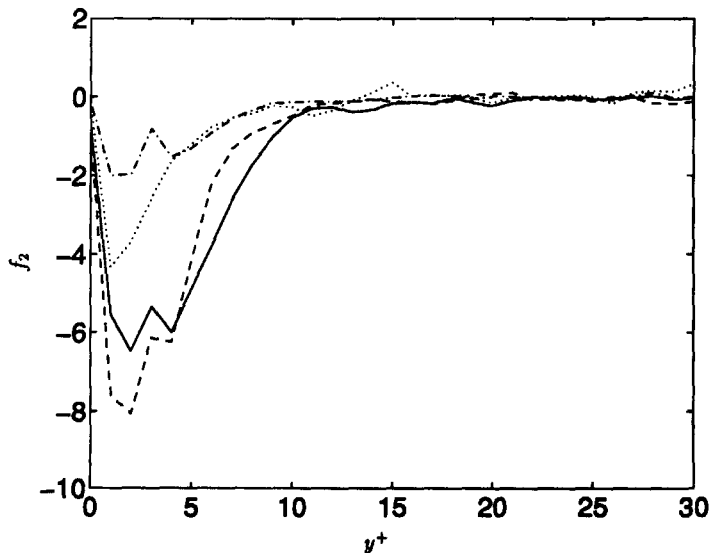


Figure 8. Comparison of the Saffman lift force and the 'optimum' lift force averaged over particles that deposit, $\rho = 713$, $Re_\tau = 180$, $\tau^+ = 6$: — Saffman; - - - optimum force; $\tau^+ = 4$: Saffman; optimum force.

It is evident that for a^+ greater than about 5, the optimum force agrees well with the empirical correlation whereas the Saffman force is smaller, especially for larger a^+ .

It should also be noted that in the forms of the lift force discussed above and used in formulation of the optimum force, the effect of particle rotation has been neglected. Cherukat and McLaughlin (1994) derived expressions for the lift force for both non-rotating and freely rotating spheres. Equation [11] used in the optimum lift force is the form for non-rotating spheres. As discussed in Cherukat and McLaughlin (1994), the differences in the expressions for rotating and non-rotating spheres can be important in some instances. However, for situations in which the lift is expected to have the largest effect (particle leading the fluid by a large slip velocity), the difference in the lift for rotating and non-rotating spheres in Cherukat and McLaughlin (1994) is small. When the particle lags the fluid, the difference between the expressions is even smaller. It is also important to note that the two expressions for the lift in Cherukat and McLaughlin (1994) yield almost the same force except when the particle is almost touching the wall. This is consistent with the experimental measurement of Cherukat and McLaughlin (1990) in which it was observed there was no rotation for particles as close as two radii from the wall and that rotation was only observed when the spheres touched the wall. More recently, Cherukat and McLaughlin (1996) carried out numerical simulations to determine the lift on a sphere in a shear flow and found that the lift on a non-rotating sphere is significantly different from that on a rotating sphere in the regime where $Re_s^{1/2} \ll Re_s$ (i.e. small ϵ). However, in this regime the magnitude of the lift force is small (c.f. figure 3) and, thus, rotation should not be expected to have a significant effect.

Finally, it is important to note that the optimum force is derived under the assumptions that the flow field is steady, the particle is moving at a constant velocity parallel to the shear flow, and that the velocity profile is linear. Results are presented in Vasseur and Cox (1976), Cox and Hsu (1977), and Hogg (1994) for parabolic velocity profiles; Hogg (1994) also considered particle motion across streamlines. The reader is referred to the recent work of Miyazaki *et al.* (1995) in which results are presented for the force on a sphere in unsteady flows.

3. SIMULATION OVERVIEW AND RESULTS

3.1. LES of turbulent channel flow

Large eddy simulation of the incompressible Navier–Stokes equations is used to obtain a description of the large scale velocity field in fully-developed turbulent channel flow. The filtered equations of motion can be expressed as

$$\frac{\partial \bar{u}_i}{\partial x_j} = 0, \quad [19]$$

$$\frac{\partial \bar{u}_i}{\partial t} + \frac{\partial}{\partial x_j} (\bar{u}_i \bar{u}_j) = -\frac{\partial \bar{p}}{\partial x_i} + \frac{1}{Re_\tau} \frac{\partial^2 \bar{u}_i}{\partial x_j \partial x_j} - \frac{\partial \tau_{ij}}{\partial x_j}, \quad [20]$$

where \bar{u}_i is the resolved velocity field and \bar{p} is the filtered pressure. Note that [19] and [20] have been nondimensionalized using the friction velocity u_τ and channel halfwidth δ . The Reynolds number $Re_\tau = \delta u_\tau / \nu$.

The filtering procedure used to obtain [20] yields the subgrid-scale (SGS) stress τ_{ij} which requires a model. The SGS stress τ_{ij} is parameterized using the dynamic eddy viscosity model of Germano *et al.* (1991). As described in Wang and Squires (1996a, b) dynamic SGS models possess a significant advantage compared to traditional closures in that information from the resolved scales is used to calculate the eddy viscosity. Therefore, *a priori* specification of model constants is not required.

The filtered equations of motion were solved using the fractional step method on a staggered grid (e.g. see Kim and Moin 1985; Perot 1993; Wu *et al.* 1995). Spatial derivatives were approximated using second-order accurate central differencing. The time advancement scheme is a mixed explicit/implicit method in which second-order Adams–Bashforth is used for advancement of the convective terms and part of the SGS stress while the Crank–Nicholson method was applied for update of the viscous terms and remainder of the SGS stress. The continuity constraint is

satisfied via solution of the Poisson equation for pressure. The Poisson equation is solved using series expansions in the streamwise and spanwise directions together with tridiagonal matrix inversion (e.g. see Williams 1969; Kim and Moin 1985).

Calculations were performed at two Reynolds numbers, $Re_\tau = 180$ and 1,000. The corresponding Reynolds numbers defined using the centerline velocity and channel halfwidth are 3,200 and 21,900, respectively; those defined using the bulk velocity and hydraulic diameter are 11,160 and 79,400, close to bulk velocity Reynolds numbers of 10,000 and 50,000 in the experiments of Liu and Agarwal (1974).

3.2. Calculation of particle trajectories

The motion of particles with material densities large compared to the fluid is considered. In this regime the drag force is substantially larger than forces associated with virtual mass, buoyancy, and history effects. The particle equation of motion can then be expressed as

$$\frac{d\mathbf{v}}{dt} = -\frac{\rho_f}{\rho_p} \frac{3}{4} \frac{C_D}{d} |\mathbf{v} - \mathbf{u}|(\mathbf{v} - \mathbf{u}) + \mathbf{f}. \quad [21]$$

In [21], \mathbf{v} is the particle velocity, \mathbf{u} is the velocity of the fluid at the particle position, and \mathbf{f} is the lift force per unit mass (directed in the wall-normal direction). The particle densities in [21] is denoted by ρ_p . Effects of nonlinear drag are incorporated through C_D and in this work an empirical relation from Clift *et al.* (1978) was used

$$C_D = \frac{24}{Re_s} [1 + 0.15 Re_s^{0.687}]. \quad [22]$$

The calculations correspond to a vertical channel in which gravity does not directly lead to deposition and therefore its effect has not been included in [21]. The lift force \mathbf{f} in [21] is expressed per unit mass and after nondimensionalizing in terms of u_τ and δ the non-zero component normal to the wall may be expressed as

$$f_2 = \frac{F_2}{\frac{4}{3} \pi (a\delta)^3 \rho_p} \frac{1}{u_\tau^2 / \delta}, \quad [23]$$

where F_2 is the dimensional force discussed in section 2.

The particle equation of motion [21] and particle displacement were time advanced using second-order Adams–Bashforth. The fluid velocity at the particle position was interpolated from the grid using fourth-order Lagrange polynomials (see Kontomaris *et al.* 1992 and Wang *et al.* 1995 for further discussion). For particles that moved out of the channel in the streamwise or spanwise directions, periodic boundary conditions were used to reintroduce it in the computational domain. Deposition was assumed to occur when a particle was within one radius of the wall. It should also be noted that the fluid velocity used in the particle equation of motion was the resolved component, i.e. the effect of subgrid-scale velocity fluctuations on particle motion have been neglected. As discussed in Wang and Squires (1996a), for the motion of particles with densities large compared to the fluid and at the moderate Reynolds numbers considered, neglect of SGS velocities is justified.

3.3. Results

LES of fully-developed turbulent channel flow was performed using the optimum lift force formulated in section 2. The trajectories of 20,000 particles were used in the simulations and statistics were obtained by averaging over 270 time units. Particles are characterized in terms of their relaxation time, expressed in wall units as $\tau^+ = 2\rho a^+ / 9$ where $\rho = \rho_p / \rho_f$. Shown in figure 8 are the wall-normal profiles of the lift force averaged over depositing particles in LES calculations performed at $Re_\tau = 180$. The profiles shown correspond to particles with $\tau^+ = 4$ and $\tau^+ = 6$ and were obtained from simulations performed using the optimum force summarized in table 1 and the Saffman formula. The forces have been averaged over both sides of the channel and over x - z planes. It is apparent that the magnitude of the Saffman force is about three times larger than the optimum lift force. It is also evident that, similar to the Saffman force, the optimum lift force is quite small for $y^+ > 10$, due to the reduction in both J^u and J^w .

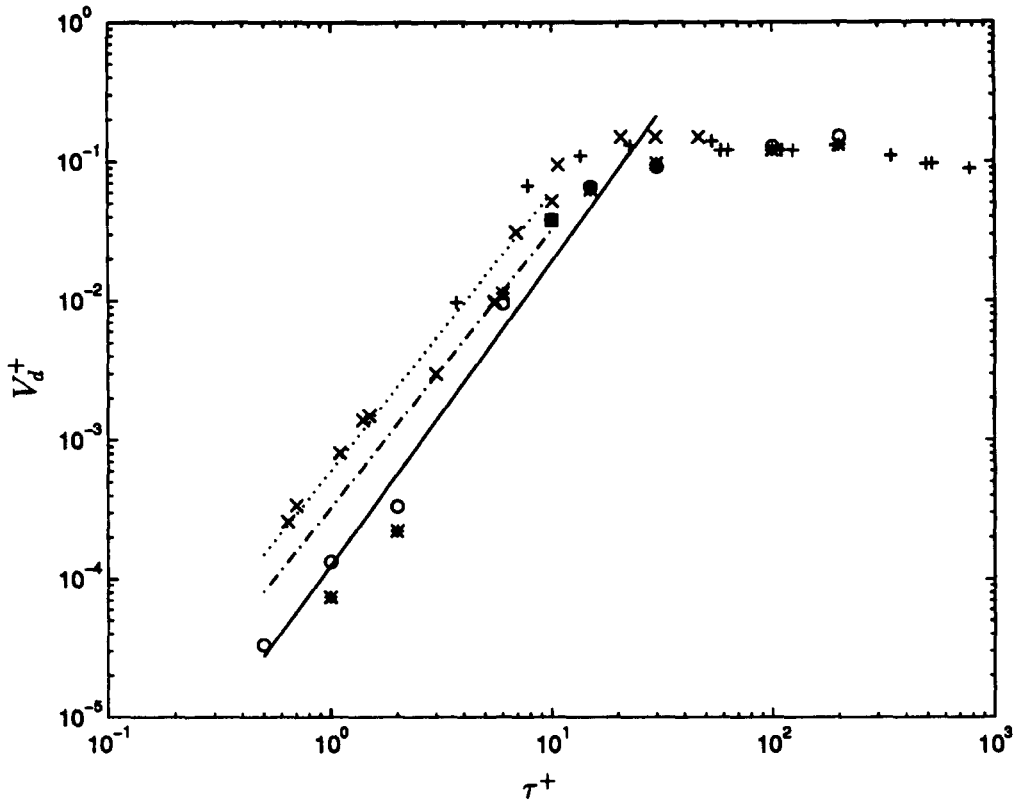


Figure 9. Particle deposition rate in turbulent channel flow, LES calculations performed using the 'optimum' lift force, $\rho = 713$ $V_d^+ = 0.0006(\tau^+)^2$ (Liu and Agarwal 1974); - · - $V_d^+ = 0.000325(\tau^+)^2$ (McCoy and Hanratty 1977). LES: \circ $Re_t = 180$; * $Re_t = 1000$; — least-squares fit of LES results; Liu and Agarwal (1974) (Reynolds numbers based on pipe diameter and average velocity): \times $Re = 10,000$; + $Re = 50,000$.

The deposition rate, defined as the ratio of the flux of particles at the deposition surface to the particle concentration, calculated using the optimum lift force in the particle equation of motion is shown in figure 9. A least-squares fit of the LES predictions yields a dependence on the relaxation time of $\tau^{+2.18}$. This is significantly smaller than the dependence obtained in simulations in which the Saffman formula was used (c.f. figure 1). The dependence of the deposition velocity on τ^+ in the LES is somewhat larger than the quadratic dependence observed experimentally. Comparing figures 9 and 1 indicates that the effect of different lift force formula on the deposition rate is largest in the range $2 < \tau^+ < 15$. Deposition rates obtained using the Saffman force are larger than those using the optimum force in this range. The predicted deposition rates are consistent with the previous discussion in that, in a typical channel flow, the Saffman force is towards the wall and possesses a larger magnitude than the optimum force.

Finally, a series of calculations were performed in which the lift force was omitted from the equation of motion. The deposition rate from these simulations is shown in figure 10. Also shown for comparison are results obtained using the optimum lift force. The results in figure 10 show that neglecting the lift force altogether affects the predicted deposition rate in the range $2 < \tau^+ < 15$. In this range deposition rates for particles with no lift are smaller than those for particles using the optimum force. This is consistent with the work of Kallio and Reeks (1989) in which the Saffman force was found to have a significant effect on deposition only for particles in the range $1 < \tau^+ < 10$. It is also interesting to note that the dependence of the deposition rate on particle relaxation time in simulations without the lift force ($V_d \sim \tau^{+1.95}$) is smaller than that obtained using the optimum lift force and in better agreement with empirical relations although the deposition rates are smaller than both those with the optimum force and those from experiments of Liu and Agarwal (1974) for intermediate τ^+ .

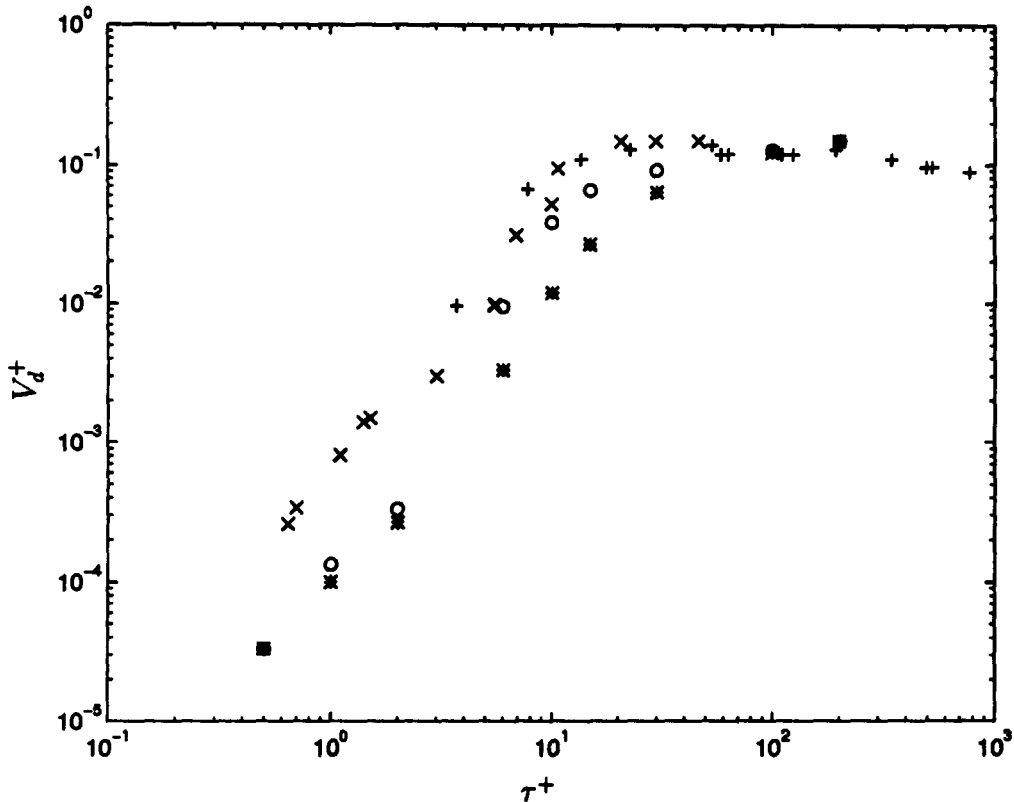


Figure 10. Comparison of particle deposition rates from simulations with no lift force to those obtained using the 'optimum' lift force, $\rho = 713$. LES; * no lift force; O 'optimum' lift force; Liu and Agarwal (1974) (Reynolds number based on pipe diameter and average velocity): \times Re = 10,000; + Re = 50,000.

4. SUMMARY

An optimum force representing the lift on a particle in a wall-bounded shear flow has been formulated which is a combination of the different forms obtained by previous investigators. The lift force is comprised of two parts: one accounting for velocity shear and the other accounting for the presence of the wall. The shear-induced part is usually smaller than that derived by Saffman (1965, 1968), and reduces to the Saffman force only in certain limiting cases. The effect of the wall on the lift, not accounted for in the Saffman formula, is significant since its effect can be larger in magnitude than the shear-induced part near the wall and may also have an opposite sign. The optimum force was incorporated into large eddy simulations of particle deposition in vertical turbulent channel flow. LES results show that the optimum lift force is substantially smaller than that obtained using the Saffman formula and results in a dependence of the particle deposition rate on relaxation time in better agreement with experiments. It was also found that the overall effect of the lift force is small since neglecting it altogether results in only a slight reduction in deposition rates compared to simulations in which it is included.

The proposed optimum lift force should find more applications in addition to the prediction of particle deposition in turbulent boundary layers. The relatively small effect of the optimum lift force on predictions of particle deposition should not be interpreted as the force itself being inaccurate or unimportant in the general case. The optimum lift force should be used rather than the Saffman force or other limiting forms derived under more restrictive conditions than surveyed in this work.

It should also be noted that, while LES results using the optimum (or no lift) force yield a dependence of the deposition rate on relaxation time in reasonable agreement with experiments, the magnitude of the deposition velocity is smaller in the LES calculations than in experiments. Some of the discrepancy can be attributed to the use of an LES, rather than a DNS. The LES requires use of a subgrid model for computation of the fluid velocity field and subgrid-scale

velocities are also not directly available for calculation of particle trajectories. Each of these contributes to the discrepancies between simulation results from LES and experimental measurements, while neither approximation is required in a DNS. Overall, however, these effects are relatively small causes for the discrepancy compared to factors such as particle polydispersity and the use of different definitions of the deposition rate, as discussed in Chen and McLaughlin (1995). Chen and McLaughlin (1995) showed that deposition rates depend strongly on particle polydispersity with monodisperse particles always having the lowest deposition rates compared to polydisperse particles. In the present work only monodisperse particles were considered and this is one cause of the under-prediction of deposition rates compared to measurements. Chen and McLaughlin (1995) also showed that the deposition rate can be increased if it is determined by weighing the deposited particle mass, rather than counting the number of deposited particles.

Finally, while the optimum lift force is considerably more appropriate for simulations of wall-bounded turbulent shear flows than the Saffman formula, the force is formally valid for spherical particles in which the Reynolds numbers are small. For depositing particles, especially those with large relaxation times, particle Reynolds numbers are often not small. Dandy and Dwyer (1990) and Mei (1992) have examined particle motion in shear flows for finite particle Reynolds numbers, although not for near-wall flows. Future efforts into generalizing the expressions for the lift to account for larger Reynolds numbers in the vicinity of a solid boundary should in turn improve the accuracy of predictions of particle deposition in turbulent boundary layers.

Acknowledgements—This work is supported by the National Institute of Occupational Safety and Health (Grant Number OH03052-03). Computer time for the simulations was supplied by the Cornell Theory Center.

REFERENCES

- Chen, M. and McLaughlin, J. B. (1995) A new correlation for the aerosol deposition rate in vertical ducts. *J. Colloid Interface Sci.* **169**, 437–455.
- Cherukat, P. and McLaughlin, J. B. (1990) Wall induced lift on a sphere. *Int. J. Multiphase Flow* **16**, 899–907.
- Cherukat, P. and McLaughlin, J. B. (1994) The inertial lift on a rigid sphere in a linear shear flow field near a flat wall. *J. Fluid Mech.* **263**, 1–18.
- Cherukat, P. and McLaughlin, J. B. (1996) Private communication from J. B. McLaughlin.
- Clift, R., Grace, J. R. and Weber, M. E. (1978) *Bubbles, Drops and Particles*. Academic Press, New York.
- Cox, R. G. and Hsu, S. K. (1977) The lateral migration of solid particles in a laminar flow near a plane. *Int. J. Multiphase Flow* **3**, 201–222.
- Dandy, D. S. and Dwyer, H. A. (1990) A sphere in shear flow at finite Reynolds number: effect of shear on particle lift, drag, and heat transfer. *J. Fluid Mech.* **216**, 381–410.
- Germano, M., Piomelli, U., Moin, P. and Cabot, W. H. (1991) A dynamic subgrid-scale eddy viscosity model. *Phys. Fluid A* **3**, 1760–1765.
- Harper, E. Y. and Chang, I.-D. (1968) Maximum dissipation resulting from lift in a slow viscous flow. *J. Fluid Mech.* **33**, 209–225.
- Hogg, A. J. (1994) The inertial migration of non-neutrally buoyant spherical particles in two-dimensional shear flows. *J. Fluid Mech.* **272**, 285–318.
- Kallio, G. A. and Reeks, M. W. (1989) A numerical simulation of particle deposition in turbulent boundary layers. *Int. J. Multiphase Flow* **15**, 433–446.
- Kim, J. and Moin, P. (1985) Application of a fractional-step method to incompressible Navier–Stokes equations. *J. Comput. Phys.* **59**, 308–323.
- Kontomaris, K., Hanratty, T. J. and McLaughlin, J. B. (1992) An algorithm for tracking fluid particles in a spectral simulation of turbulent channel flow. *J. Comput. Phys.* **103**, 231–242.
- Lilly, D. K. (1992) A proposed modification of the Germano subgrid-scale closure method. *Phys. Fluid A* **4**, 633–635.
- Liu, B. Y. H. and Agarwal, J. K. (1974) Experimental observation of aerosol deposition in turbulent flow. *Aerosol Science* **5**, 145–155.

- McCoy, D. D. and Hanratty, T. J. (1977) Rate of deposition of droplets in annular two-phase flow. *Int. J. Multiphase Flow* **3**, 319–331.
- McLaughlin, J. B. (1989) Aerosol particle deposition in numerically simulated channel flow. *Phys. Fluid A* **1**, 1211–1224.
- McLaughlin, J. B. (1991) Inertial migration of a small sphere in linear shear flows. *J. Fluid Mech.* **224**, 261–274.
- McLaughlin, J. B. (1993) The lift on a small sphere in wall-bounded linear shear flows. *J. Fluid Mech.* **246**, 249–265.
- McLaughlin, J. B. (1994) Numerical computation of particle-turbulence interaction. *Int. J. Multiphase Flow* **20**, 211–232.
- Mei, R. (1992) An approximate expression for the shear lift force on spherical particles at finite Reynolds numbers. *Int. J. Multiphase Flow* **18**, 145–147.
- Miyazaki, K., Bedeaux, D. and Bonet Avalos, J. (1995) Drag on a sphere in slow shear flow. *J. Fluid Mech.* **296**, 373–390.
- Perot, J. B. (1993) An analysis of the fractional step method. *J. Comput. Phys.* **108**, 51–58.
- Saffman, P. G. (1965) The lift on a small sphere in a slow shear flow. *J. Fluid Mech.* **22**, 385–340.
- Saffman, P. G. (1968) Corrigendum to ‘The lift on a small sphere in a slow shear flow’. *J. Fluid Mech.* **31**, 624.
- Vasseur, P. and Cox, R. G. (1976) The lateral migration of a spherical particle in two-dimensional shear flows. *J. Fluid Mech.* **78**, 385–418.
- Vasseur, P. and Cox, R. G. (1977) The lateral migration of a spherical particles sedimenting in a stagnant bounded fluid. *J. Fluid Mech.* **80**, 561–591.
- Wang, Q. and Squires, K. D. (1996a) Large eddy simulation of particle deposition in a vertical turbulent channel flow. *Int. J. Multiphase Flow* **22**, pp. 667–683.
- Wang, Q. and Squires, K. D. (1996b) Large eddy simulation of particle-laden turbulent channel flows. *Phys. Fluids* **8**, 1207–1223.
- Wang, Q., Squires, K. D. and Wu, X. (1995) Lagrangian statistics in turbulent channel flow. *Atmospheric Environment* **29**, 2417–2427.
- Williams, G. P. (1969) Numerical integration of the three-dimensional Navier–Stokes equations for incompressible flow. *J. Fluid Mech.* **37**, 727–750.
- Wu, X., Squires, K. D. and Wang, Q. (1995) On extension of the fractional step method to general curvilinear coordinate systems. *Numerical Heat Transfer* **27**, 175–194.